

Experimental Study of Corona Jet Produced from a Circular Tube Fitted with a Nozzle

I. W. Brindle and F. C. Lai
School of Aerospace and Mechanical Engineering
University of Oklahoma, Norman
phone: (1) 405-325-1748
email: flai@ou.edu

Abstract—The flow characteristics of a corona jet, which is produced from a single needle electrode positioned at the centerline of a circular tube fitted with a grounded stainless steel nozzle at one end of the tube, is experimentally evaluated. Six nozzles with two diameter ratios and three taper angles are evaluated for their effectiveness in accelerating the jet produced by corona discharge with positive polarity. To determine the maximum jet velocity and volume flow rate, experiments have been conducted at a voltage ranging from corona onset (5 kV) to sparkover (approximately 12.5 kV) at an increment of 2.5 kV. The results show that the jet velocity increases with the applied voltage. The maximum velocity occurs at the center line but its value decreases as the jet expands downstream. In addition, the results show that a nozzle with a smaller diameter ratio does not always perform the best in accelerating the flow or producing the maximum volume flow rate. The nozzle's taper angle further accentuates the result produced by the diameter ratio. The implications from the present results for actual applications are provided.

I. INTRODUCTION

Corona discharge is a natural phenomenon which has attracted great attention for decades. It can also be produced manually and has many important engineering applications. To produce the discharge manually, it requires two electrodes with different curvature. By applying a high voltage (usually in the kilovolt range) to pin-like or wire-like emitting electrode, the electric field near the electrode is intensified. When its strength is greater than the dielectric strength of air, air molecules close to the electrode break down and become ionized. The ions are driven by Coulomb force and migrate to the grounded electrode. Along the way, the momentum of ions is transferred to neutral molecules through collision, which produces additional ions pairs and leads to the generation of corona wind. The drifted ions are then collected by the grounded electrode and output an electric current (in the microampere to milliamper range).

Corona wind generated from the process described above can put to good use in many engineering applications [1]. For example, it has been employed in electrostatic

precipitators (ESPs) for the control of particle emission in power industry as well as cement plants [2]. Since corona discharge produces low temperature plasma, it can be used for food dehydration process [3-5] to keep the nutrients from thermal degradation due to high temperature. A plasma actuator embedded on airfoil can also be used for flow control to put off the flow separation point that leads to drag reduction [6-9]. In recent years, the technology based on the electrohydrodynamics (EHD) has become one of the promising technologies in removing heat from a targeted area [10-11], especially from those of miniaturized electronic devices which generate tremendous heat flux in operation. It utilizes the ionic wind generated from corona discharge to perturb the momentum and thermal boundary layers over a heated surface [12]. The traditional heat removal techniques, such as forced convection by fan or natural convection through fins, proves insufficient in such application. In addition to the application in heat transfer enhancement, EHD technique has been widely applied to other fields [13]. Another important application of EHD technique is gas pumping. An EHD gas pump has no moving component, thus no noise induced by vibration. In addition, its operation can be easily controlled by varying the electric field. While the applied voltage may be high, the current involved is usually small, which makes its power consumption considerably insignificant. This has become one of the most attractive features for EHD technique. In recent years, there sees a surge of interest in the application of EHD technique for pumping dielectric liquids [12]. Because of their low power consumption and no moving part, EHD pumps have been considered a valuable alternative for conventional pumps.

A variety of EHD gas pumps have been studied in recent years. These include using electrode configurations of pin-plate [14], wire-rod [15, 16], wire-plate [17-21], and needle-mesh [22]. Among these studies, Zhao and Adamiak [14] examined the flow field produced by a corona wind generator with pin-plate configuration. Their results show that the wind velocity increases to a highest value near emitting electrode, and decreases radially away from electrode. Their results also show recirculation induced by EHD jet flow. Komeili, et al. [16] investigated the flow induced by an EHD gas pump with wire-rod geometry. They reported that the induced air velocity increased with the rod diameter for a fixed pipe diameter and electrode spacing. However, they suggested to use a rod electrode with a smaller diameter for the consideration of power consumption. Tsubone et al. [18] studied the characteristics of flows produced by an EHD gas pump with wire-plate configuration. Because of the similarity between an EHD flow and a jet flow, they observed the presence of turbulent eddies and small scale recirculation at low Reynolds numbers. Chang, et al. [19] used wire as the emitting electrode and non-parallel plates as the grounded electrode to study the effect of the position of emitting electrode on the resulting flow direction. Their results showed that the flow direction could be manipulated by changing the position of electrodes. Tsubone et al. [20] studied the flows produced by an EHD gas pump with wire and non-parallel plate configuration in a converging cone. Their result shows no obvious change in pressure at the upstream of emitting electrode but it increases at the downstream of emitting electrode. Chang et al. [21] studied the electric discharge and flow characteristics of an EHD gas pump with the same electrode configuration as that used in [20]. However, their emphasis was on placed on the effect of converging angle formed by the plates. An increase in the air velocity and pressure was reported when the channel converging angle was 3 degrees. When the an-

gle became greater than 3 degrees, recirculating flow was observed inside the channel. As a result, a greater flow resistance was encountered when the converging angle increased (i.e., a smaller exit area). Zhang and Lai [23] conclude and point out that higher applied voltage does not necessarily enhance the efficiency of gas pump, instead, resulting in more power consumption. The possible reason is that the resistance caused by the formation of recirculation flow at certain operated condition.

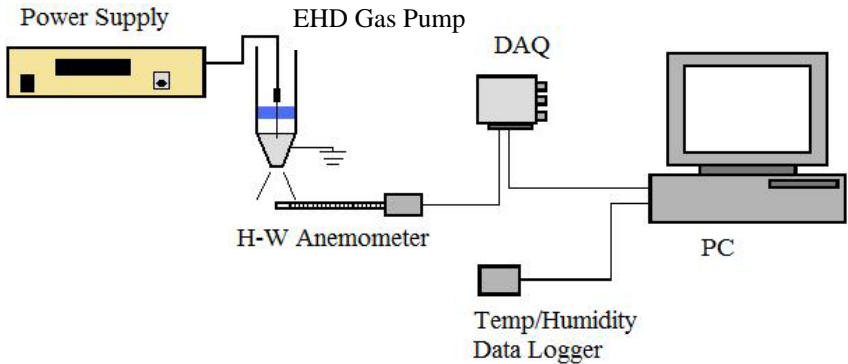
Rickard, et al. [24] studied the flow produced by an EHD gas pump with and without a nozzle attached at the exit of the pump. Their results showed that only a slight increase in velocity could be achieved by adding a converging nozzle downstream of the electrodes. It is worthwhile to mention that they used both hotwire anemometry and particle image velocimetry (PIV) to measure corona jet velocity in their study. They noted that seed-based measurement techniques (such as PIV) were complicated by the charging of seed particles. As seed particles entrained through the region of corona discharge, they got charged causing them to deviate from the flow streamlines under the influence of Coulomb force. The flow characteristics of a single stage cylindrical EHD gas pump with four emitting electrodes was studied by Brown and Lai [25]. They noted that operating an EHD pump at a higher applied voltage does not necessarily improve its performance, but rather simply increases its power consumption. Most importantly, they noticed that the volume flow rate appeared to approach an asymptotic value as the applied voltage increased before sparkover. Recently, Birhane et al. [26] extended the study of Brown and Lai [23] to examine the flow characteristics of an EHD pump with eight emitting electrodes. They confirmed the previous finding by Brown and Lai [25] that there exists a maximum volume flow rate that a single-stage EHD pump can deliver before the occurrence of sparkover.

For some applications, it is desirable to have a corona jet at a higher velocity. Although this can usually be accomplished through increasing the applied voltage, it has been shown that the jet velocity would reach an asymptotic value before sparkover occurs. Also, it has been shown that it is not energy efficient to operate an EHD gas pump at a high voltage. As such, an alternative approach is required for meeting the need. To this end, previous studies have considered non-parallel plate [18-21] or nozzle [24] with varying degree of success. However, additional studies are required to fully understand the electrical discharge and flow characteristics involved in these devices. The motivation of this study is to examine the performance of an EHD gas pump in a circular tube fitted with a nozzle. Different from the previous study [24], the present study uses the nozzle as the ground electrode directly.

II. EXPERIMENTAL SETUP AND PROCEDURE

The schematic of the experimental setup used in this study is shown in Fig. 1(a). The EHD gas pump is installed in a circular Plexiglas tube. The tube has a 2-inch outer diameter and 0.25-inch wall thickness. The pump uses a sharp needle as the emitting electrode and a nozzle which is attached at the end of the tube as the ground electrode. The needle is a standard sewing needle which has a diameter of 1.168 mm. The needle is held in the centerline of the tube by a plastic holder made by 3D printing using Acryloni-

trile Butadiene Styrene (ABS) thermoplastic resin as the material (Fig. 1(b)). To accommodate the needle holder, the tube is made in two parts. The top part is fabricated with a 0.25-inch indentation to accommodate the electrode holder and the bottom part with the same indentation on one side and a threaded section on the other side for the attachment of nozzle. The two parts of the tube are left separated for the ease of manufacturing; they are assembled and secured by electrical tape before experiment. Six nozzles (Fig. 2(a)) which are different in their diameter ratio and taper angle are tested. Table 1 details the values selected for diameter ratio and taper angle for this study. For the ease of assembly, the outer wall of the nozzle inlet is threaded. The length of the threaded section is 10.5 mm. Since the inlet diameter of the nozzle is fixed, the diameter ratio and taper angle alone can completely define the nozzle in use (Fig. 2(b)). The nozzles are fabricated from 304 stainless steel for their ease of manufacturing and good electrical properties. The electrode spacing (d) is defined as the distance between the needle tip and the inlet of the nozzle that is below the threaded portion. Two electrode spacings are considered in this study. One is fixed at 10.5 mm (i.e., the needle tip is at the same level of the nozzle inlet), the other 0 mm (i.e., the needle tip is at the same level of the nozzle thread end). Unless specified otherwise, it is fixed at 10.5 mm.



(a)



(b)

Fig. 1 (a) Schematic of experimental setup, (b) assembly of emitting electrode.

Table 1. Parameters for the nozzles tested.

Nozzle #	Diameter Ratio	Taper Angle (Deg)
1	0.2	15
2	0.2	20
3	0.2	30
4	0.4	15
5	0.4	20
6	0.4	30

The present setup is different from that used by Rickard, et al. [24] in that the nozzle has been used as the ground electrode directly without additional metal ring to serve the same purpose. In addition, the velocity of the corona jet produced is measured in-situ downstream of the nozzle exit without re-directing the flow to a separate measuring spot using a rubber tubing. In this case, the accuracy of the measurement would not be compromised by the frictional loss through the tubing.

To generate corona wind, a high voltage power supply (Bertan Series 205B) is connected to the emitting electrodes. The power supply has a maximum voltage of 30 kV and an accuracy of 0.1 kV. Although the power supply can produce direct current in both positive or negative polarity, it has been observed that corona discharge with negative polarity is less stable during experimentation and thus only the results obtained from positive polarity are presented in the present study. Both the nozzle and power supply were grounded to the same level for consistency. A multimeter (FLUKE 287) is used to measure the corona current on the grounded plate of the EHD gas pump. It has an accuracy of $\pm 1V$ in voltage and 2% in current. A hot-wire anemometer by Omega (model FMA 902-I) was used for the measurement of the corona wind velocity. The hotwire anemometer can accurately measure air velocity up to 2.54 m/s with an accuracy of 2.7% of full scale at room temperature. The acquired signal is transferred to a data acquisition

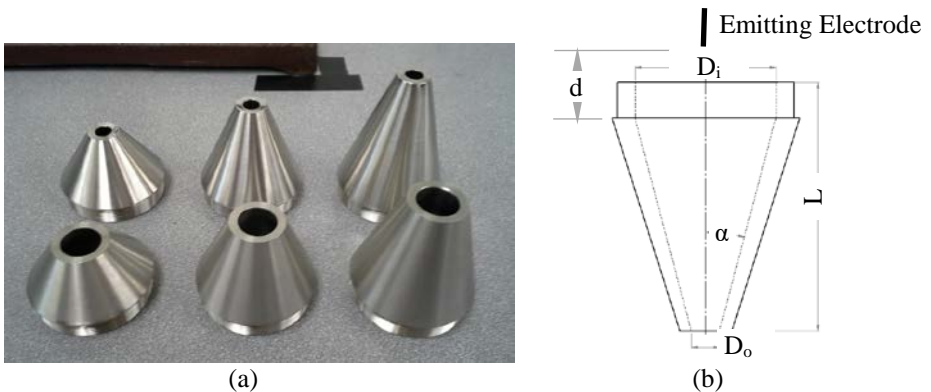


Fig. 2 (a) Nozzles, (b) dimensions of nozzle.

system (DAQ) by National Instrument and is converted to velocity by LabView program. The velocity probe extended horizontally allowing measurements to be taken on three levels; 10, 20, and 50 mm below the exit of the nozzle. At each level, velocities were measured radially outward from the centerline of the nozzle at an increment of 3 mm. It has been observed that the corona jet produced is nearly axi-symmetrical. With an increase in the axial distance from the nozzle exit, the jet width increases. As such, the number of the sampling points is also increased proportionally to get a detailed profile of the corona jet. The uncertainty associated with the measurements was calculated by the method proposed by Steele et al. [27]. Since air temperature and humidity can significantly affect corona discharge, they are closely monitored using Dickson temperature and humidity datalogger (D200) during the experiment and are maintained within 55~62%, and 20~23 °C, respectively.

III. RESULTS AND DISCUSSION

A typical set of voltage-current characteristics of the EHD pumps examined is shown in Fig. 3. The voltage-current characteristics remain nearly the same for all nozzle configurations considered with a maximum discrepancy on the order of 0.01 mA. It is shown that the corona current increases in a relatively quadratic trend as the applied voltage increases. Note that the maximum applied voltage was kept at 12.5 kV in the present study due to the limitation on the maximum measurable velocity of the hot-wire anemometer.

After partially ionized, air is discharged through nozzle to the ambient. Because of the reduction in the cross-sectional area along the flow path, air is accelerated when it is discharged to the ambient. Ideally, it would take the form of a round jet with the maximum velocity at the centerline of the nozzle. The jet spreads radially outward as it moves downstream. Figure 4 shows the velocity profile at the three different levels downstream from the nozzle exit. As observed, the velocity decreases radially outward from

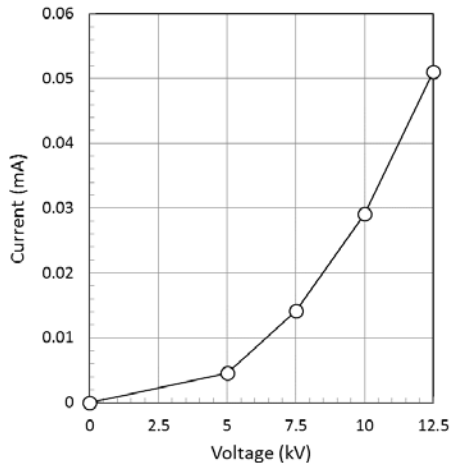


Fig. 3 Voltage-current characteristic curves of the EHD gas pumps.

the centerline and, as the distance from the nozzle increases, the maximum velocity also decreases. Note that Figure 4 only displays the velocity profile for a jet width of 20 mm at each level. It should be expected that each nozzle would have a different velocity profile and thus a different jet width. For the present study, the width of a corona jet is defined by the velocity measurement at which the jet velocity becomes less than 0.1 m/s. The jet width produced by each nozzle is presented in Fig. 5 for an applied voltage of 10 kV. As shown, nozzles with a diameter ratio of 0.4 generally have a larger jet width closer to the outlet, but the width does not increase as significantly as those with a diameter ratio of 0.2. Also, as the taper angle decreases, the jet width decreases which indicates that nozzles with a larger taper angle tend to spread wider. This indicates that a nozzle with a smaller diameter ratio and a smaller taper angle produces a more concentrated jet which may not travel as far as jets produced by other nozzles.

The effect of electrode spacing can be examined from Fig. 6 where the centerline velocity of the corona jet produced by Nozzle #2 (which has a diameter ratio of 0.2 and a taper angle of 20°) is presented for various applied voltages. First, one should note that the maximum applied voltage before sparkover increases as the electrode spacing increases. This is mainly due to the weakening of the electric field strength as the gap distance between electrodes increases. In this case, one observes that the threshold voltage of sparkover changes from 14.2 kV to 16.3 kV when the electrode spacing changes from $d = 0$ mm to 10.5 mm. As shown in the figure, the centerline velocity decreases as the distance from the nozzle exit increases, which can also be observed from the velocity profiles presented in Fig. 4. Also observed, as d increases, the outlet velocity decreases proportionally, a trend that has also been observed in the previous study [28].

The centerline velocities of corona jets produced by nozzles at various applied voltages are shown in Fig. 7. In general, one observes that the centerline velocity increases as

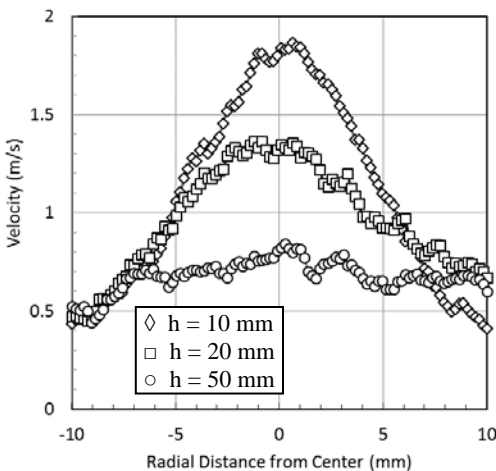


Fig. 4 Velocity profile at various downstream distances from the nozzle exit (Nozzle #2 with an applied voltage of positive polarity at 10 kV).

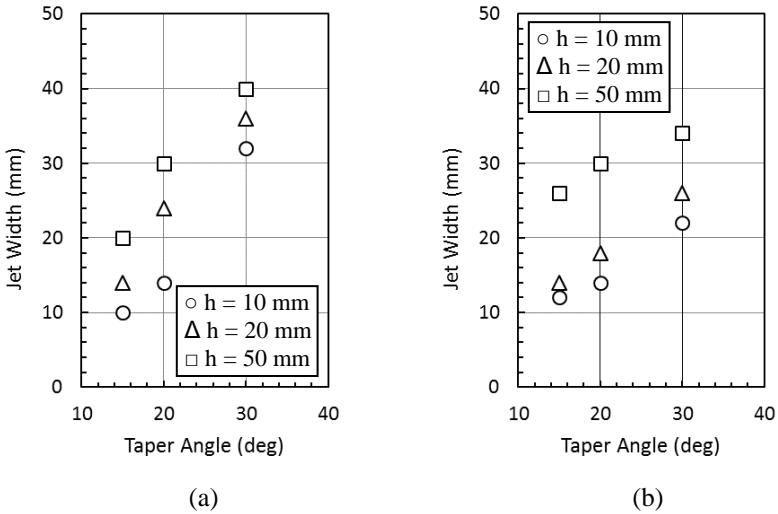


Fig. 5 Variation of jet width with the taper angle of nozzle, (a) DR = 0.2, (b) DR = 0.4.

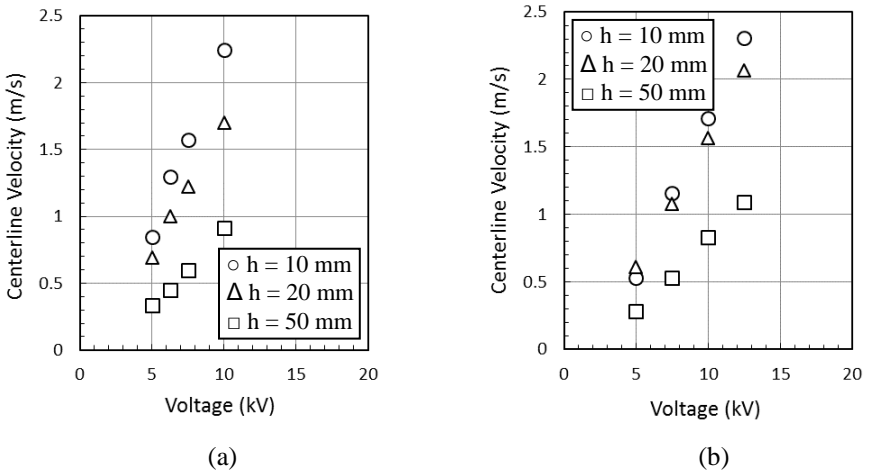


Fig. 6 Centerline velocity of corona jet at various downstream distances from the nozzle exit (Nozzle #2, DR = 0.2, $\alpha = 20^\circ$), (a) $d = 0$ mm, (b) $d = 10.5$ mm.

the applied voltage increases. Also observed, the centerline velocity increases with an increase in the nozzle diameter ratio (i.e., a smaller contraction in the cross-sectional area) for a given applied voltage. Clearly, a nozzle with a smaller diameter ratio leads to flow restructuring inside the nozzle and thus a greater pressure loss. In addition, one observes that the centerline velocity further increases with an increase in the taper angle of the nozzle. This may first seem to contradict to one's intuition. However, it can be explained as follows. For the present study, the nozzle inlet diameter is fixed. As such, a

smaller taper angle implies a longer nozzle length, which adversely increases the pressure loss for the corona jet to pass through the nozzle and thus leads to a reduction to the centerline velocity. Especially for a nozzle with a smaller diameter ratio, it experiences a steeper reduction in the centerline velocity. The present result is not to be confused with the result reported by Chang et al. [21], which was conducted using non-parallel plates (which can be thought of as a planar nozzle). They observed that when the converging angle is greater than 3 degrees, recirculating flow was formed inside the channel which led to a greater flow resistance. The difference between their study and the current one is that the channel length is fixed in the former study so that an increase in the converging angle is equivalent to an increase in the cross-sectional area ratio (or in terms of the present study, the diameter ratio). So, there is no contradiction between the two results. Also, it is worthwhile to point out that Rickard, et al. [24] also studied the flow produced by an EHD gas pump with a nozzle attached to the exit of the pump. Their results showed that the air velocity has a limiting value regardless of the exit-to-inlet area ratio (i.e., the diameter ratio of the nozzle). The present results may seem to contradict theirs as well. However, a closer look at their experimental setup, one notices that the velocity measurement in their study was not performed in-situ, but rather at a distance further downstream of the nozzle exit. The corona jet produced by their EHD gas pump was routed to the sampling site using a rubber tubing. Clearly the pressure restriction caused by the rubber tubing has compromised their results.

The volume flow rates produced by the EHD gas pump with six different nozzles are shown in Fig. 8. As observed, all volume flow rates increase with the applied voltage, but they are significantly less than that produced by the same EHD gas pump without a nozzle. Also observed is that the taper angle has a greater influence over the volume flow rate for the EHD pump fitted with a nozzle of a small diameter ratio. On the other

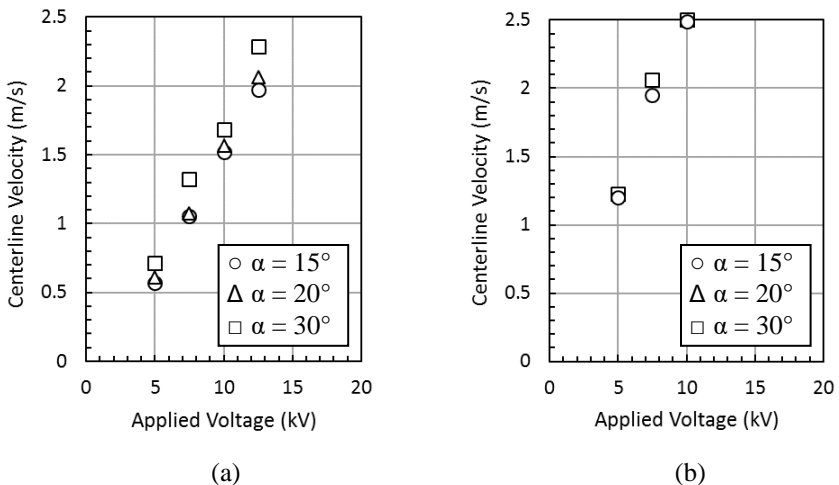


Fig. 7 Centerline velocities of corona jets produced by nozzles at various applied voltages (at 20 mm downstream from the nozzle exit), (a) DR = 0.2, (b) DR = 0.4.

hand, the EHD pump with a large diameter ratio (such as $DR = 0.4$), the effect of taper angle on the volume flow rate is almost insignificant. As discussed earlier, flow restructuring takes place when the diameter ratio of the nozzle decreases. A small taper angle adversely leads to a longer nozzle length and increases the pressure loss. Consequently, pressure loss due to flow restructuring becomes more significant for nozzles with a smaller diameter ratio.

Since the maximum (centerline) velocity and volume flow rate are the two most important outputs from an EHD gas pump, two criteria related to these two quantities are used in the evaluation of the performance of the EHD gas pump considered. One is the acceleration factor and the other volume flow rate factor, which are defined below,

$$AF = \frac{V}{V_0}, \quad (1)$$

$$QF = \frac{Q}{Q_0}, \quad (2)$$

where V and Q are respectively the centerline velocity and volume flow rate produced by the EHD pump fitted with a nozzle while V_0 and Q_0 are their counter parts without nozzle.

The acceleration factors of the six nozzles considered are shown in Fig. 9. It is interesting to note that the nozzle diameter ratio has a very significant effect on the acceleration factor. For the EHD gas pump fitted with a nozzle having a diameter ratio of 0.2, the acceleration factor is always less than unity while that with a diameter ratio of 0.4 is

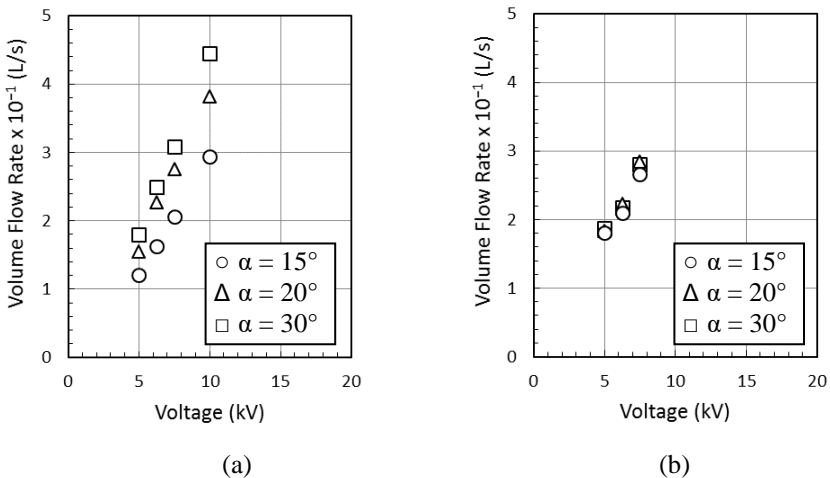


Fig. 8 Volume flow rates produced by the EHD gas pump examined, (a) $DR = 0.2$, (b) $DR = 0.4$.

always greater than one. This implies that a large contraction in the nozzle exit area does not always produce the desired result in accelerating the flow. Because of the flow restructuring inside the nozzle, it may even produce a counter effect. In this case, the EHD gas pump fitted with a nozzle of DR = 0.2 produces a jet velocity that is less than that without a nozzle at all. Particularly, a nozzle with a smaller taper angle makes the result even worse (Fig. 9(a)). On the other hand, for the EHD gas pump with a nozzle of DR = 0.4, the results are more encouraging in that the jet velocity is always greater than that without a nozzle. However, one should note that in all cases, the acceleration factor decreases with an increase in the applied voltage, which implies that the pressure loss due to flow restructuring inside the nozzle increases with the applied voltage and compromises the result desired.

The volume flow rates factors of the six nozzles considered are shown in Fig. 10. It is observed that for all cases considered, the volume flow rate factor is less than unity, which means that the EHD gas pump fitted with a nozzle produces less volume flow rate than that without a nozzle. It may not be a surprise for the EHD pump fitted with a nozzle of DR = 0.2 since the centerline (maximum) velocity it produces is less than that for an EHD pump without nozzle (Fig. 9(a)). However, for the EHD pump fitted with a nozzle of DR = 0.4, even though its centerline velocity is greater than that for an EHD pump without nozzle (Fig. 9(b)), its average velocity is still less than the latter and thus leads to a smaller volume flow rate. As the applied voltage increases, the volume flow rate reduces further. Clearly, this is a significant penalty one has to pay when fitting an EHD gas pump with a nozzle.

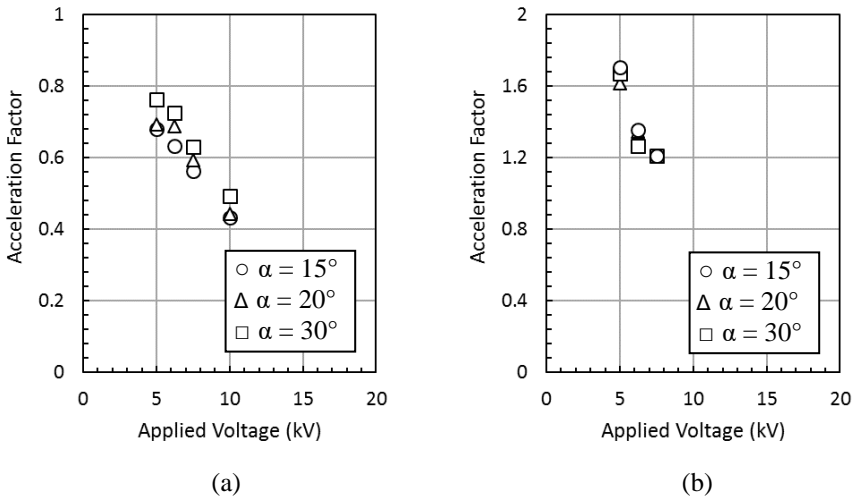


Fig. 9 Acceleration factors of the six nozzles examined, (a) DR = 0.2, (b) DR = 0.4.

IV. CONCLUSION

Experiments have been conducted to study the characteristics of flow produced by an EHD gas pump fitted with a nozzle. The result shows that the performance of the pump is greatly influenced by the diameter ratio and taper angle of the nozzle. Particularly, it shows that a reduction in the diameter ratio and taper angle of the nozzle leads to flow restructuring inside the nozzle and thus does not always produce the effect that one desires. This has an important implication for the application of EHD gas pump. The main purpose for one to fit an EHD gas pump with a nozzle is to accelerate the flow produced. As the present result revealed, this can be generally achieved through a proper choice of the diameter ratio of the nozzle. However, a smaller diameter ratio does not always lead to a significant increase in the jet velocity. In some cases (such as the case of $DR = 0.2$ in the present study), it even produces a counteracting result. In addition, the nozzle's taper angle can further accentuate the result produced by the diameter ratio. Therefore, one needs to verify the result before actual application. One also needs to bear in mind that a nozzle even is effective in accelerating the flow produced by the EHD pump, it comes with a significant price tag of reduced volume flow rate.

While the present study has explored the performance of an EHD gas pump fitted with a nozzle, the complicated relation between the pump performance and nozzle geometry still awaits further investigation. In search for a better solution in applications, the authors feel that a multi-stage EHD gas pump may be more viable from the viewpoint of efficient use of energy. As the authors have shown in their previous work of multi-stage EHD gas pumps, the latter can increase (or at least sustain) the volume flow rate that they

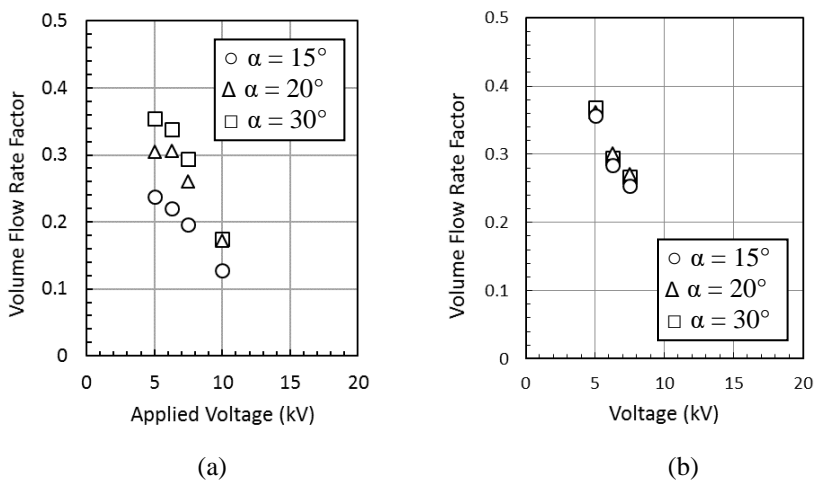


Fig. 10 Volume flow rate factors of the six nozzles examined, (a) $DR = 0.2$, (b) $DR = 0.4$.

produced over a longer distance. However, when an EHD gas pump fitted with a nozzle is really in need for a specific application, one needs to carefully study the relation between the pump performance and the nozzle geometry as it may not be as straightforward as one would expect judging from the results obtained from the present study.

REFERENCES

- [1] Fylladitakis, E. D., Theodoridis, M. P., and Moronis, A. X., "Review on the History, Research, and Applications of Electrohydrodynamics," *IEEE Transactions on Plasma Science*, Vol. 42, pp. 358-375, 2014.
- [2] Yamamoto, T., and Velkoff, H. R., "Electrohydrodynamics in an Electrostatic Precipitator," *Journal of Fluid Mechanics*, Vol. 108, pp. 1-18, 1981.
- [3] Cao, W., Nishiyama, Y., and Koide, S., "Electrohydrodynamic Drying Characteristics of Wheat Using High Voltage Electrostatic Field," *Journal of Food Engineering*, Vol. 62, pp. 209-213, 2004.
- [4] Basiry, M., and Esehaghbeygi, A., "Electrohydrodynamic (EHD) Drying of Rapeseed (*Brassica napus* L.)," *Journal of Electrostatics*, Vol. 68, pp. 360-363, 2010.
- [5] Esehaghbeygi, A., and Basiry, M., "Electrohydrodynamic (EHD) Drying of Tomato Slices (*Lycopersicon Esculentum*)," *Journal of Food Engineering*, Vol. 104, pp. 628-631, 2011.
- [6] Suzen, Y. B., Huang, P. G., Jacob, J. D., and Ashpis, D. E., "Numerical Simulations of Plasma Based Flow Control Applications," 35th AIAA Fluid Dynamics Conference and Exhibit, AIAA Paper 2005-4633, 2005.
- [7] Suzen, Y. B., Huang, P. G., and Ashpis, D. E., "Numerical Simulations of Flow Separation Control in Low-Pressure Turbines Using Plasma Actuators," 45th AIAA Aerospace Sciences Meeting and Exhibit, AIAA Paper 2007-937, 2007.
- [8] Touchard, G., "Plasma Actuators for Aeronautics Applications – State of Art Review," *International Journal of Plasma Environmental Science and Technology*, Vol. 2, pp. 1-25, 2008.
- [9] Ashpis, D., and Thurman, D., "DBD Plasma Actuators for Flow Control in Air Vehicles and Jet Engines—Simulation of Flight Conditions in Test Chambers by Density Matching," 42nd AIAA Plasmadynamics and Lasers Conference, AIAA Paper 2011-3730, 2011.
- [10] Jewell-Larsen, N. E., Ran, H., Zhang, Y., Schwiebert, M. K., Tessera, K. A. H., and Mamishev, A. V., "Electrohydrodynamic (EHD) Cooled Laptop," *Proceedings of IEEE 25th Annual Semiconductor Thermal Measurement and Management Symposium, SEMI-THERM 2009*, pp. 261-266, 2009.
- [11] Huang, R.-T., Sheu, W.-J., and Wang, C.-C., "Heat Transfer Enhancement by Needle-Arrayed Electrodes – An EHD Integrated Cooling System," *Energy Conversion and Management*, Vol. 50, pp. 1789-1796, 2009.
- [12] Robinson, M., "Convective Heat Transfer at the Surface of a Corona Electrode," *International Journal of Heat and Mass Transfer*, Vol. 13, pp. 263-274, 1970.
- [13] Seyed-Yagoobi, J., "Electrohydrodynamic Pumping of Dielectric Liquids," *Journal of Electrostatics*, Vol. 63, pp. 861-869, 2005.
- [14] Zhao, L., and Adamiak, K., "EHD Flow in Air Produced by Electric Corona Discharge in Pin-Plate Configuration," *Journal of Electrostatics*, Vol. 63, No. 3-4, pp. 337-350, 2005.
- [15] Komeili, B., Chang, J.-S., Harvel, G. D., Ching, C. Y., and Brocilo, D., "Flow Characteristics of Wire-Rod Type Electrohydrodynamic Gas Pump under Negative Corona Operations," *Journal of Electrostatics*, Vol. 66, pp. 342-353, 2008.
- [16] Takeuchi, N., Yasuoka, K., and Chang, J.-S., "Wire-Rod Type Electrohydrodynamic Gas Pumps with and without Insulation Cover over Corona Wire," *IEEE Transactions on Dielectrics and Electrical Insulation*, Vol. 18, pp. 801-808, 2011.
- [17] Leger, L., Moreau, E., and Touchard, G., "Effect of a DC Corona Electrical Discharge on the Airflow along a Flat Plate," *IEEE Transactions on Industry Applications*, Vol. 38, pp. 1478-1485, 2002.
- [18] Tsubone, H., Ueno, J., Komeili, B., Minami, S., Harvel, G. D., Urashima, K., Ching, C. Y., and Chang, J.-S., "Flow Characteristics of DC Wire-Non-Parallel Plate Electrohydrodynamic Gas Pumps," *Journal of Electrostatics*, Vol. 66, pp. 115-121, 2008.
- [19] Chang, J.-S., Ueno, J., Tsubone, H., Harvel, G. D., Minami, S., and Urashima, K., "Electrohydrodynamically Induced Flow Direction in a Wire-Non-Parallel Plate Electrode Corona Discharge," *Journal of Physics D, Applied Physics*, Vol. 40, pp. 5109-5111, 2007.

- [20] Tsubone, H., Chang, J.-S., Harvel, G. D., and Urashima, K., "Non-Moving Component Pumping of Narrow Gas Flow Channels by an Electrohydrodynamic Gas Pumps," *International Journal of Plasma Environmental Science and Technology*, Vol. 3, pp. 151-155, 2009.
- [21] Chang, J.-S., Tsubone, H., Chun, Y. N., Berezin, A. A., and Urashima K., "Mechanism of Electrohydrodynamically Induced Flow in a Wire-Non-Parallel Plate Electrode Type Gas Pump," *Journal of Electrostatics*, Vol. 67, pp. 335-339, 2009.
- [22] Qiu, W., Xia, L., Tan, X., and Yang, L., "The Velocity Characteristics of a Serial-Staged EHD Gas Pump in Air," *IEEE Transactions on Plasma Science*, Vol. 38, pp. 2848-2853, 2010.
- [23] Zhang, J., and Lai, F. C., "Effect of Emitting Electrode Number on the Performance of EHD Gas Pump in a Rectangular Channel," *Journal of Electrostatics*, Vol. 69, pp. 486-493, 2011.
- [24] Rickard, M., Dunn-Rankin, D., Weinberg, F., and Carleton, F., "Characterization of Ionic Wind Velocity," *Journal of Electrostatics*, Vol. 63, pp. 711-716, 2005.
- [25] Brown, N. M., and Lai, F. C., "Electrohydrodynamic Gas Pump in a Vertical Tube," *Journal of Electrostatics*, Vol. 67, pp. 709-714, 2009.
- [26] Birhane, Y. T., Lin, S. C., and Lai, F. C., "Flow Characteristics of a Single Stage EHD Gas Pump in Circular Pipe," *Journal of Electrostatics*, Vol. 76, pp. 8-17, 2015.
- [27] Steele, W. G., Taylor, R. P., Burrell, R. E., and Coleman, H. W., "Use of Previous Experience to Estimate Precision Uncertainty of Small Sample Experiments," *AIAA Journal*, Vol. 31, pp. 1891-1896, 1993.
- [28] Mazumder, A. K. M. M. H., and Lai, F. C., "Enhancement in Gas Pumping in a Square Channel with Two-stage Corona Wind Generator," *IEEE Transactions on Industry Applications*, Vol. 50, pp. 2296-2305, 2014.